

Efficient Sodium Cation Transport Across Liposome Membranes Using Synthetic Carriers

Qingshan Xie, Yi Li, George Gokel, Jeanette Hernández, and Luis Echegoyen*

Contribution from the Department of Chemistry, University of Miami, Coral Gables, Florida 33124

Received August 20, 1993*

Abstract: A series of 12 synthetic ionophores containing an amide substituent connected via a methylene bridge to an aza-crown ring were evaluated for their ability to transport Na^+ across large unilamellar vesicles (LUVs) using dynamic ^{23}Na NMR spectroscopy. The structures contain lipophilic groups connected to the amide nitrogen, ranging in size from C_3H_{11} to $\text{C}_{18}\text{H}_{37}$, and are either tertiary or secondary amides. The crown ether ring size was also varied from 12-C-4 to 15-C-5 to 18-C-6. Surprisingly, the Na^+ transport efficiencies were very high, with one synthetic system exhibiting an overall transport rate constant similar to that for a naturally-occurring ionophore, monensin. The value of k_2 was $2.1 \times 10^4 \text{ s}^{-1}$ for $(18\text{N})\text{CH}_2\text{CON}(\text{C}_{10}\text{H}_{21})_2\text{-Na}^+$, which compares with $2.0 \times 10^4 \text{ s}^{-1}$ for monensin- Na^+ . The overall transport rate efficiency followed the same trend as that of the binding abilities of the ligands. In every case, the 18-C-6 derivatives were more effective transporters than their 15-C-5 analogues, which in turn were better than the 12-C-4's. Ligands containing a secondary instead of a tertiary amide substituent were always poorer transporters. Homonuclear ^1H NOESY conclusively showed that this is due to the formation of an intramolecular H-bond between the amidic proton and the polyether ring. The Na^+ transport mechanism, determined here for the first time for a synthetic ionophore in a bilayer environment, was shown to be controlled by diffusion of the complex across the bilayer. The value of k_{diff} determined for $(15\text{N})\text{CH}_2\text{CON}(\text{C}_{10}\text{H}_{21})_2\text{-Na}^+$ was $3.2 \times 10^3 \text{ M s}^{-1}$.

Introduction

Since their conception, substituted macrocyclic polyethers have been modified primarily with the intent to enhance cation binding while retaining a high degree of kinetic lability of the corresponding complexes in order to mimic biological ion carriers.¹ Many crown ethers have been prepared with a wide variety of functional groups, while the macroring sizes have also been varied.² Different degrees of cation-binding enhancement and transport rates have been obtained while the overall flexibility of the resulting metal cation complexes has been shown to be retained.³ The net effect has been an increase in cation transport rates, at least across bulk liquid model membranes.⁴

There are many reports related to the cation-transporting abilities of naturally-occurring ionophores incorporated directly into lipid bilayer membranes.⁵ Some of the specific systems that have been studied in this category include monensin,⁶ antibiotic M139603,⁷ salinomycin,⁸ narasin,⁸ and nigericin.⁹ Most of these have been evaluated in large unilamellar vesicles (LUVs) using dynamic NMR techniques and magnetization transfer experiments by Riddell and his co-workers.⁵⁻⁹ Details of their transport model and their interpretation of results are presented later.

* Abstract published in *Advance ACS Abstracts*, December 15, 1993.

(1) Fyles, T. M. In *Bioorganic Chemistry Frontiers, Vol 1*; Dugas, H., Ed.; Springer-Verlag: Berlin, 1990; p 71.

(2) Izatt, R. M.; Bradshaw, J. S.; Nielsen, S. A.; Lamb, J. D.; Christensen, J. J. *Chem. Rev.* **1985**, *85*, 271.

(3) Gokel, G. W.; Trafton, J. E. In *Cation Binding by Macrocycles*; Inoue, Y., Gokel, G. W., Eds.; Marcel-Dekker: New York, 1990; p 253.

(4) (a) Lamb, J. D.; Izatt, R. M.; Garrick, D. G.; Bradshaw, J. S.; Christensen, J. J. *J. Membr. Sci.* **1981**, *9*, 83. (b) Izatt, R. M.; Izatt, S. R.; McBride, D. W., Jr.; Bradshaw, J. S.; Christensen, J. J. *Isr. J. Chem.* **1985**, *25*, 27. (c) Dulyea, L. M.; Fyles, T. M.; Whitfield, D. M. *Can. J. Chem.* **1984**, *62*, 498.

(5) Riddell, F. G. *Chem. Br.* **1992**, 533.

(6) (a) Riddell, F. G.; Hayer, M. K. *Biochim. Biophys. Acta* **1985**, *817*, 313. (b) Riddell, F. G.; Arumugam, S.; Cox, B. G. *J. Chem. Soc., Chem. Commun.* **1987**, 1890. (c) Riddell, F. G.; Arumugam, S. *Biochim. Biophys. Acta* **1988**, *945*, 65.

(7) Riddell, F. G.; Arumugam, S. *Biochim. Biophys. Acta* **1989**, *984*, 6.

(8) Riddell, F. G.; Tompssett, S. J. *Biochim. Biophys. Acta* **1990**, *1024*, 193.

(9) Riddell, F. G.; Arumugam, S.; Brophy, P. J.; Cox, B. G.; Payne, M. C. H.; Southon, T. E. *J. Am. Chem. Soc.* **1988**, *110*, 734.

Interestingly, the number of reports of cation transport mediated by synthetic ionophores in lipid bilayer systems is extremely limited.¹⁰ Synthetic ionophores have typically been evaluated using model liquid membranes, both bulk liquid membranes¹¹ and solid-supported liquid membranes.¹² One would assume that, after the high degree of maturity achieved by the synthetic ionophore field, work using liposomal membranes would be commonplace. This is unfortunately not the case. It is unfortunate because it has been shown that the cation transport mechanism can be different when it is measured across a lipid bilayer than when it is observed across a model liquid membrane.⁵⁻⁹ For example, Riddell et al. have shown that the kinetics of cation transport mediated by the anionic natural ionophores monensin, nigericin, salinomycin, M139603, and narasin across liposomal bilayers are always controlled by the dissociation rate constant of the complex, not by diffusion across the bilayer.⁵⁻⁹ On the other hand, cation transport kinetics measured across liquid membranes (bulk or solid-supported) always result in a process that is controlled by diffusion of the complex across the membrane phase.¹³ It is thus important to evaluate the cation transport kinetics and to elucidate the corresponding mechanisms using synthetic ionophores across liposomal bilayers if their potential as antibiotics is ever to be assessed. At best, cation transport

(10) (a) Kobuke, Y.; Yamamoto, J.-Y. *Bioorg. Chem.* **1990**, *18*, 283. (b) Thomas, C.; Sauterey, C.; Castaing, M.; Gary-Bobo, C. M.; Lehn, J.-M.; Plumere, P. *Biochem. Biophys. Res. Commun.* **1983**, *116*, 981. (c) Castaing, M.; Morel, F.; Lehn, J.-M. *J. Membr. Biol.* **1986**, *89*, 251. (d) Shinar, H.; Navon, G. *J. Am. Chem. Soc.* **1986**, *108*, 5005. (e) Carmichael, V. E.; Dutton, P. J.; Fyles, T. M.; James, T. D.; Swam, J. A.; Zojaji, M. *J. Am. Chem. Soc.* **1989**, *111*, 767. (f) Kragten, U. F.; Roks, M. F. M.; Nolte, R. J. M. *J. Chem. Soc., Chem. Commun.* **1985**, 1275.

(11) (a) Reusch, C. F.; Cussler, E. L. *AIChE J.* **1973**, *736*. (b) Lamb, J. D.; Christensen, J. J.; Izatt, S. R.; Bedke, K.; Astin, M. S.; Izatt, R. M. *J. Am. Chem. Soc.* **1980**, *102*, 3399. (c) Lamb, J. D.; Christensen, J. J.; Oscarson, J. L.; Nielsen, B. L.; Asay, B. W.; Izatt, R. M. *J. Am. Chem. Soc.* **1980**, *102*, 6820. (d) Kobuke, Y.; Hanji, K.; Horiguchi, K.; Asada, M.; Nakayama, Y.; Furukawa, J. *J. Am. Chem. Soc.* **1976**, *98*, 7414. (e) Kirch, M.; Lehn, J.-M. *Angew. Chem., Int. Ed. Engl.* **1975**, *14*, 555.

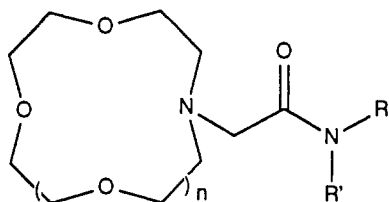
(12) For a recent example see: Nijenhuis, W. F.; Buitenhuis, E. G.; de Jong, F.; Sudhölter, E. J. R.; Reinhoudt, D. N. *J. Am. Chem. Soc.* **1991**, *113*, 7963.

(13) (a) Behr, J.-P.; Kirch, M.; Lehn, J.-M. *J. Am. Chem. Soc.* **1985**, *107*, 241. (b) Fyles, T. *J. Membr. Sci.* **1985**, *24*, 229.

studies across bulk liquid membranes have tenuous biological relevance. To our knowledge, no work has been reported for synthetic cation carriers in lipid bilayers in an attempt to elucidate the mechanistic details. Very few reports have appeared for synthetic carriers incorporated into lipid bilayers,¹⁰ and none of these have addressed the mechanistic details to decide if the overall cation transport process is controlled by binding, diffusion of the complex, or release of the cation. This report represents the first time that these questions have been directly addressed for a series of synthetic cation carriers.

Ligands containing amide substituents have been shown to be particularly good binders.¹⁴ This is so because the highly negative amide oxygen is able to provide considerable stabilization to the cation complexes formed. ¹³C NMR and cation transport experiments were recently reported for a series of bibrachial lariat ethers, some of which contained amide groups as side arms.¹⁴ In this work, the amide carbonyl was removed from the macroring nitrogens by a methylene spacer. ¹³C NMR shifts were reported for these ligands upon addition of several cations and interpreted in terms of solution structure and dynamic behavior.¹⁴ This work made no reference to the possibility of intramolecular H-bonding interactions between the amide hydrogen and the macroring polyether oxygens. However, such interactions were discussed in the case of some lariat ethers where the amide substituents were directly connected to the polyether ring.^{15,16}

The systems reported here contain monoaza-crown ethers with lipophilic side arms connected to an amide functionality. The amide functionality is connected to the macroring nitrogen via a methylene spacer. The general structure is given. The crown



rings used had $n = 1, 2, \text{ or } 3$, and R and R' were varied between C_5H_{11} and $\text{C}_{18}\text{H}_{37}$. Secondary amides were also investigated where R = lipophilic chain and R' = H. Their Na^+ transport properties in liposomes have been explored here using dynamic ²³Na NMR. Cation transport rates across bulk liquid membranes for these compounds were already reported.¹⁷

General Description and Kinetic Model

In order to have a simple nomenclature for the compounds studied while keeping relatively informative names, the same scheme as that used in ref 17 was adopted here. The symbol $\langle 00N \rangle$ is used to represent an aza-lariat ether having 00 atoms in the macroring. Side arms attached to the macroring nitrogen are explicitly written following the ring identifier. Thus, $\langle 15N \rangle\text{-CH}_2\text{CON}(\text{C}_5\text{H}_{11})_2$ stands for the compound with $n = 2$, $\text{R} = \text{R}' = -(\text{C}_5\text{H}_{11})$.

General Description of Experiments. LUVs were prepared from L- α -phosphatidylcholine (PC) and L- α -phosphatidylglycerol (PG), 10:1 mol ratio, following the method of Szoka and Papahadjopoulos^{18a} or by the dialytic detergent removal technique introduced by Reynolds et al.^{18b} Results were nearly independent of which technique was used to constitute the LUVs, confirming

(14) (a) Tsukube, H. *J. Chem. Soc. Perkin Trans. 1* **1989**, 89. (b) Tsukube, H. *J. Chem. Soc. Perkin Trans. 1* **1989**, 1537.

(15) (a) Behr, J.-P.; Lehn, J.-M.; Vierling, P. *Helv. Chim. Acta* **1982**, 65, 1853. (b) Behr, J.-P.; Lehn, J.-M. *J. Am. Chem. Soc.* **1981**, 103, 701.

(16) Behr, J.-P.; Lehn, J.-M. *Nature* **1982**, 295, 526.

(17) Hernández, J. C.; Trafton, J. E.; Gokel, G. W. *Tetrahedron Lett.* **1991**, 6269.

(18) (a) Szoka, F., Jr.; Papahadjopoulos, D. *Proc. Natl. Acad. Sci. U.S.A.* **1978**, 75, 4194. (b) Mimms, L. T.; Zamphigi, G.; Nozaki, Y.; Tanford, C.; Reynolds, J. A. *Biochemistry* **1981**, 20, 833.

the near quantitative incorporation of the lipids into LUVs in both cases. Their size distributions were established using light-scattering techniques.¹⁹ A typical preparation consisted of vesicles with an average diameter of 180 ± 60 nm. The standard deviations were consistently small, indicating relatively narrow distributions in all cases. LUVs were constituted in a medium containing 0.12 M Na^+ so that intra- and extraventricular concentrations were identical. For most experiments, the carriers were added to the vesicle suspensions via direct injection of a relatively concentrated chloroform solution. However, in some cases the lipophilic carrier was directly incorporated into the liposomes during their preparation, in order to ensure their presence in the lipid bilayer. This was the case for $\langle 12N \rangle\text{CH}_2\text{CON}(\text{C}_{18}\text{H}_{37})_2$, $\langle 15N \rangle\text{CH}_2\text{CON}(\text{C}_{18}\text{H}_{37})_2$, and $\langle 18N \rangle\text{CH}_2\text{CON}(\text{C}_{18}\text{H}_{37})_2$. It was only necessary for these three compounds since, due to their extremely low water solubility, it was almost impossible to add them to the membrane of the liposomes after these had been constituted. This is a situation which is not normally recognized or appreciated by many who look for the highest possible lipophilicity of the carriers used. While high lipophilicity will keep the carrier in the membrane and avoid losses to the surrounding aqueous medium (a most desired situation), it will inhibit incorporation of such molecules if added to an already prepared liposome suspension. Direct incorporation versus addition after formation of the liposomes did not have an effect for the compounds with tails shorter than C_{18} . Since kinetic measurements derived from dynamic NMR experiments as described here are conducted under equilibrium situations, addition versus direct incorporation of the carrier during liposome preparation should have no effect on the final results.

Once the liposomes were formed and the synthetic carriers were incorporated in the membranes, an aqueous shift reagent was added to the solution, dysprosium tripolyphosphate, $\text{Na}_7\text{-Dy}(\text{PPP})_2$, generated in situ by the reaction between $\text{Na}_5(\text{PPP})$ and DyCl_3 .²⁰ This shift reagent generates a 7 ppm separation between the Na^+ resonance inside the liposomes (Na^+_{in}) and that outside (Na^+_{out}), the latter being shifted upfield relative to the former. In the presence of an effective carrier, both of these ²³Na⁺ resonance signals broaden as a result of exchange, which is typically in the slow exchange region.⁵⁻⁹

Kinetic Model. In the slow exchange region it is well-known that the rate constant, $k (=1/\tau)$, is directly proportional to the line broadening observed, $(\Delta\nu - \Delta\nu_0)$, where $\Delta\nu$ is the line width at half-height of the observed resonance line in the presence of carrier and $\Delta\nu_0$ is the corresponding value in the absence of carrier, eq 1. If the line width is measured for the M^+_{in} resonance in the

$$k = 1/\tau = \pi[(\Delta\nu - \Delta\nu_0)] \quad (1)$$

series of dynamic NMR spectra, then the rate obtained is that for efflux of M^+ from the vesicles. Since the rate constants are a function of the concentrations of the carriers and of the PC, the rate constants must be normalized by dividing the measured values by $[\text{L}]_{\text{T}}$, where $[\text{L}]_{\text{T}} = [\text{L}]/[\text{PC}]$. An additional correction to the rate constant must be applied in the present case due to the fact that the PC vesicles prepared contained some phosphatidylglycerol (PG), thus altering the percent volume enclosed by these.^{6c} No effort was made to quantify the effect of the negative charge introduced by the PG on the transport rates, but all of the results are consistent. Transport rates across vesicle systems are a function of their size, *vide infra*.^{6c} Although all of the cases studied here used the same phospholipid composition and thus the results were internally consistent, they cannot be directly compared to those of others, unless a volume correction is applied to the rate constants. Therefore, the normalized rate values were multiplied by the percent volume enclosed by the

(19) Zumbuhl, O.; Weder, H. G. *Biochim. Biophys. Acta* **1981**, 640, 252.

(20) Gupta, R. K.; Gupta, P. *J. Magn. Reson.* **1982**, 47, 344.

PC-PG liposomes and divided by that which would have resulted from preparation of the vesicles with PC only.^{6c} After these corrections, results can be directly compared to those of others. Most results presented here were conducted at a constant $[Na^+] = 120$ mM. Variable $[Na^+]$ studies were conducted in only one case, in order to probe the mechanistic details of the overall transport process, *vide infra*. It was considered that the mechanism observed for one member of this closely related family of compounds would reflect the behavior of the complete series.

The model used to interpret the mechanistic details has been presented by Riddell and co-workers⁵⁻⁹ and is essentially the same as that originally developed by Painter and Pressman.²¹ In this model, cation complexation and decomplexation (characterized by rate constants k_f and k_d , respectively) occurs between the membrane-bound carrier and the aqueous cation at both bilayer-water interfaces. Diffusion of the complex across the membrane is characterized by another rate constant, k_{diff} . The rate equation derived from this model is eq 2

$$1/\tau_{M^+,in} = \{Ak_{diff}k_d[L]_T\}/\{V_{in}(k_d + 2k_{diff})([M^+] + k_d/k_f)\} \quad (2)$$

where τ is the lifetime of a metal ion inside a vesicle with volume V_{in} and surface area A . Equation 2 can be rewritten as

$$1/\tau_{M^+,in} = (A/V_{in})\{V_m[L]_T/(K_m + [M^+])\} = k_2[L]_T \quad (3)$$

where $K_m = k_d/k_f = K_s^{-1}$ and the value of V_m depends on k_{diff} and k_d . K_s is the apparent stability constant of the carrier-cation complex in the membrane. Plots of the normalized rate constants determined from the line widths vs $[M^+]$ yield straight lines with slopes equal to $1/V_m$ and intercepts equal to K_m/V_m . Therefore, the ratio of slope to intercept is K_s for the membrane-bound complex. These conditions are always met if the kinetic model can be directly applied to the carrier-mediated transport process.

There are two limiting cases under which eq 2 can be simplified, one where the overall kinetic transport process is controlled by slow diffusion of the complex across the lipid bilayer ($k_d \gg k_{diff}$) and the other where dissociation of the complex is rate limiting ($k_{diff} \gg k_d$). Under these two conditions, eq 2 simplifies to eqs 4 and 5, respectively. As previously mentioned, cation transport

$$1/\tau_{M^+,in} = (A/V_{in})(k_{diff}[L]_T)/([M^+] + k_d/k_f) \quad \text{if } k_d \gg k_{diff} \quad (4)$$

$$1/\tau_{M^+,in} = (A/V_{in})(k_d[L]_T)/2([M^+] + k_d/k_f) \quad \text{if } k_{diff} \gg k_d \quad (5)$$

mediated by anionic naturally-occurring ionophores has always resulted in the observation of a process that is kinetically controlled by complex dissociation, not by diffusion across the bilayer.⁵⁻⁹ Thus eq 5 has been shown to describe the behavior of naturally-occurring cation carriers.

Experimental Section

Materials. PC and PG (Sigma Chemical Co.) were purchased as chloroform solutions and used without further purification. An NaCl (Sigma Chemical Co.) solution was prepared with water that was deionized using a Barnstead Nanopure system to a resistance of 18 M Ω . The sodium salt of the anionic shift reagent (dysprosium triphosphate) was synthesized in situ by the reaction of DyCl₃-H₂O (Alfa) and sodium triphosphate (Sigma) following the procedure described in ref 20.

Vesicle Preparation. LUVs were prepared from a 10:1 mixture of PC:PG by the reverse-phase evaporation technique described in detail by Szoka and Papahadjopoulos^{18a} or by the detergent removal technique introduced by Reynolds et al.^{18b} In a typical preparation, 125 μ mol of PC and 12 μ mol of PG were used in order to produce approximately 4 mL of the LUV suspension. All aqueous environments, inside and outside

of the vesicles, contained 120 mM NaCl and were buffered to pH 8.2 using a phosphate system. Filtration of the LUV preparation through 0.4- μ m polycarbonate membranes (Nuclepore Corp.) resulted in a reasonably homogeneous population of liposomes and no appreciable lipid residue. These averaged 180 nm in diameter. Analyses of these suspensions using ²³Na NMR spectroscopy indicated that the average volume entrapment ratio was 0.2.

²³Na NMR Measurements. Two milliliters of the liposome suspension was placed in a 10-mm-i.d. NMR sample tube, and 40 μ L of 0.25 M Na₇Dy(PPP)₂ was added to induce a 6-7 ppm shift difference between the resonances corresponding to Na⁺_{in} and Na⁺_{out}. The solution was then allowed to equilibrate in the refrigerator overnight before data acquisition.

In the usual case, where the carrier was added to the vesicle suspension as a chloroform solution, the stock solution was typically 20 mM. Microliter amounts of this solution were then added to the 2 mL of the vesicle suspension directly in the NMR sample tube. The sample was then gently agitated by slow bubbling of either Ar or N₂ for 10 min and allowed to equilibrate an additional 30 min before insertion into the NMR probe for analyses. For the carriers possessing C₁₈H₃₇ substituents it was necessary to mix the ligands directly with the phospholipids in the initial step of vesicle preparation. It was found that this method, direct incorporation, was very effective for all ligands, but only strictly necessary for those cases with the highest lipophilicity.

²³Na NMR spectra were recorded at 23.65 MHz using a JEOL FX-90Q spectrometer at room temperature. The instrument was internally locked on the ²H resonance of ²H₂O, which was placed in a coaxial 5-mm tube within the 10-mm sample. Typically, 1000 FIDs were collected using 512 data points and a sweep width of 1000 Hz. The FIDs were zero filled and transformed as 4K data sets. Spectra were line broadened, typically by 1 Hz, to improve the signal-to-noise ratio. $\Delta\nu$ was measured directly from the spectra at half-height of the ²³Na resonances.

¹H NMR Measurements. All ¹H NMR spectra were acquired using a Varian VXR-400 spectrometer, operating at 399.852 MHz. Typically, ¹H NMR spectra were acquired using 40K data points and zero filled to 80K. Line broadening of 0.5 Hz was used for all ¹H NMR spectra. NOESY spectra were acquired using a 1K by 512 data matrix and later zero filled to 1K by 1K. A mixing time of 0.5 s and a pulse delay of 1.0 s were used for all experiments.

Results and Discussion

A typical ²³Na⁺ dynamic NMR spectral sequence is presented in Figure 1 for $\langle^{15}N\rangle CH_2CON(C_{10}H_{21})_2$ acting as a carrier. The spectra in Figure 1 were obtained at constant $[Na^+]$ while increasing $[L]_T$. Notice that both resonances, corresponding to Na⁺_{in} and Na⁺_{out}, broaden as a result of increasing the carrier concentration, as expected. The broadening is more pronounced for the Na⁺_{in} resonance since the amount of intravesicular Na⁺ is smaller than the extravesicular one, due to the relatively small percentage of encapsulated volume, which is approximately 20%. It must be stressed that the actual Na⁺ concentration inside and outside the vesicles is identical. Using the broadening observed for the Na⁺_{in} resonance, the rate constants were determined using eq 1.

Normalized rate constants for Na⁺ transport across the vesicle membrane are summarized in Table 1. Entries can be found for all of the 12 synthetic compounds studied here, along with one for monensin and one for a model system, $\langle^{18}N\rangle C_{18}H_{37}$. The latter was included in order to assess the transporting ability of a lipophilic 18-crown-monoaza ring system without the amide functionality attached. Na⁺ transport was measured for the naturally-occurring ionophore monensin in order to calibrate the method and to compare, under identical experimental conditions, with the results obtained with the synthetic carriers. Note that the value measured for monensin, 2.0×10^4 s⁻¹ is close to that calculated from one of Riddell's reports, 2.5×10^4 s⁻¹.^{6a} This value was not directly reported in ref 6a, but enough information was provided in this reference to calculate this value following the description above. The only information that was not available was the volume data, so it was not possible to apply a proper volume correction to the measured rate constant. Thus, the

(21) Painter, G. R.; Pressman, B. C. *Top. Curr. Chem.* **1982**, *101*, 83.

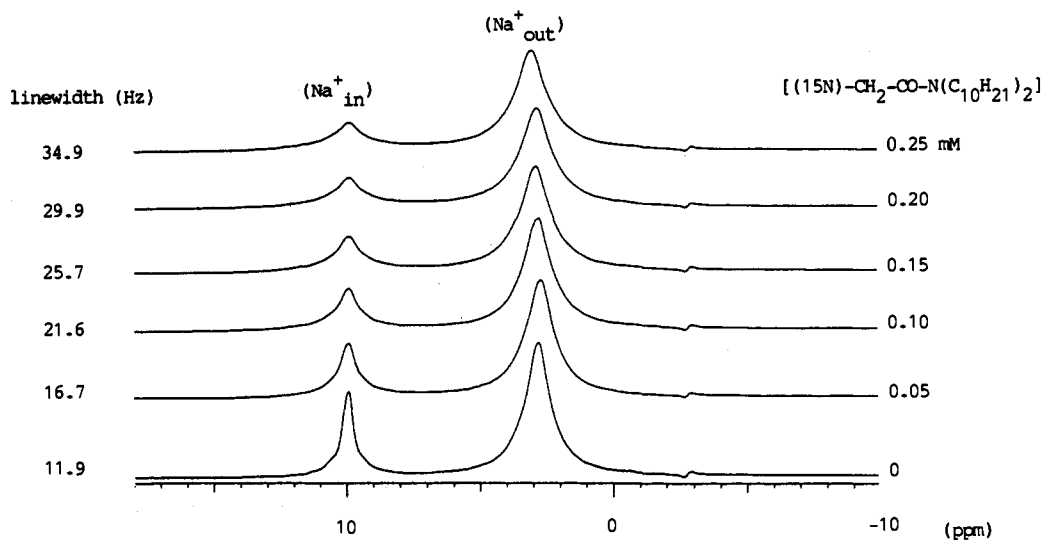


Figure 1. Typical dynamic ^{23}Na NMR spectra showing the effect of increasing the $[(15\text{N})\text{CH}_2\text{CON}(\text{C}_{10}\text{H}_{21})_2]$ in a liposome preparation containing 120 mM $[\text{Na}^+]$. Notice how both Na^+_{in} and Na^+_{out} resonances broaden as the carrier concentration increases.

Table 1. Normalized Transport Rate Constants^a and Binding Constants for Sodium

carrier	$\log K_s(\text{Na}^+)^{17}$	$[\text{L}]_{\text{T}}^b$	k (1/s) ^c	$k_2(10^4)^d$
$\langle 12\text{N} \rangle \text{CH}_2\text{CON}(\text{C}_5\text{H}_{11})_2$	3.32	$3.2\text{e-}3$	11.0	0.34
$\langle 12\text{N} \rangle \text{CH}_2\text{CON}(\text{C}_{18}\text{H}_{37})_2$	3.42	$3.2\text{e-}3$	21.3	0.66
$\langle 15\text{N} \rangle \text{CH}_2\text{CON}(\text{C}_5\text{H}_{11})_2$	4.20	$3.2\text{e-}3$	35.7	1.11
$\langle 15\text{N} \rangle \text{CH}_2\text{CONH}(\text{C}_5\text{H}_{11})_2$	3.09	$3.2\text{e-}3$	12.1	0.38
$\langle 15\text{N} \rangle \text{CH}_2\text{CON}(\text{C}_{10}\text{H}_{21})_2$	4.35	$3.2\text{e-}3$	40.5	1.27
$\langle 15\text{N} \rangle \text{CH}_2\text{CONH}(\text{C}_{10}\text{H}_{21})_2$	3.04	$3.2\text{e-}3$	22.7	0.70
$\langle 15\text{N} \rangle \text{CH}_2\text{CON}(\text{C}_{18}\text{H}_{37})_2$	4.10	$3.2\text{e-}3$	30.1	0.93
$\langle 18\text{N} \rangle \text{CH}_2\text{CON}(\text{C}_5\text{H}_{11})_2$	4.61	$3.2\text{e-}3$	40.6	1.26
$\langle 18\text{N} \rangle \text{CH}_2\text{CON}(\text{C}_{10}\text{H}_{21})_2$	4.71	$3.2\text{e-}3$	66.5	2.06
$\langle 18\text{N} \rangle \text{CH}_2\text{CONH}(\text{C}_{10}\text{H}_{21})_2$	3.63	$3.2\text{e-}3$	39.5	1.22
$\langle 18\text{N} \rangle \text{CH}_2\text{CON}(\text{C}_{18}\text{H}_{37})_2$	4.58	$3.2\text{e-}3$	59.5	1.84
$\langle 18\text{N} \rangle \text{CH}_2\text{CONH}(\text{C}_{18}\text{H}_{37})_2$	3.64	$3.2\text{e-}3$	35.4	1.10
$\langle 18\text{N} \rangle (\text{CH}_2)_{17}\text{CH}_3$	3.53	$3.2\text{e-}3$	4.2	0.13
monensin	4.90 ²	$3.2\text{e-}3$	63.2	1.96

^a In all cases, $[\text{Na}^+]$ is 120 mM. ^b $[\text{L}]_{\text{T}} = [\text{carrier}]/[\text{PC}]$. ^c Rate constant after volume correction. ^d $k_2 = k/[\text{L}]_{\text{T}}$.

method used here to determine the rate constants is perfectly consistent with those reported by others.⁵⁻⁹

There is one striking result in this table that immediately calls attention. The Na^+ transport rate by $\langle 18\text{N} \rangle \text{CH}_2\text{CON}(\text{C}_{10}\text{H}_{21})_2$ is $2.1 \times 10^4 \text{ s}^{-1}$. This indicates that under the equilibrium transport conditions employed in this study, Na^+ transport efficiency by a naturally-occurring ionophore is matched by that of this synthetic carrier. This unanticipated result was checked via independent experiments with the same carrier at least three times. It was also internally confirmed by the values obtained for the other 18-membered ring compounds, which were also very efficient Na^+ carriers under the present conditions. Thus for example, $\langle 18\text{N} \rangle \text{CH}_2\text{CON}(\text{C}_{18}\text{H}_{37})_2$ exhibits a transport rate of $1.8 \times 10^4 \text{ s}^{-1}$ and $\langle 15\text{N} \rangle \text{CH}_2\text{CON}(\text{C}_{10}\text{H}_{21})_2$ exhibits a value of $1.3 \times 10^4 \text{ s}^{-1}$, which are relatively close to the value exhibited by monensin. The lowest transport rate observed for an amide-substituted carrier was that for $\langle 12\text{N} \rangle \text{CH}_2\text{CON}(\text{C}_5\text{H}_{11})_2$, at a value of $0.34 \times 10^4 \text{ s}^{-1}$. The system without an amide substituent, $\langle 18\text{N} \rangle \text{C}_{18}\text{H}_{37}$, was even lower at $0.13 \times 10^4 \text{ s}^{-1}$.

Every compound studied exhibits a linear relationship between the observed transport rate and the concentration of carrier used in the experiment. Such observations are consistent with the model described above and indicates a first-order relationship between the carrier concentration and the transport rate. Thus, a 1:1 carrier: Na^+ complex is involved in all cases. Two typical plots are shown together in Figure 2, for the cases of $\langle 15\text{N} \rangle \text{CH}_2\text{CON}(\text{C}_{10}\text{H}_{21})_2$ and $\langle 15\text{N} \rangle \text{CH}_2\text{CON}(\text{C}_5\text{H}_{11})_2$. A slight curvature is observed in the cases where the amide side arm contains

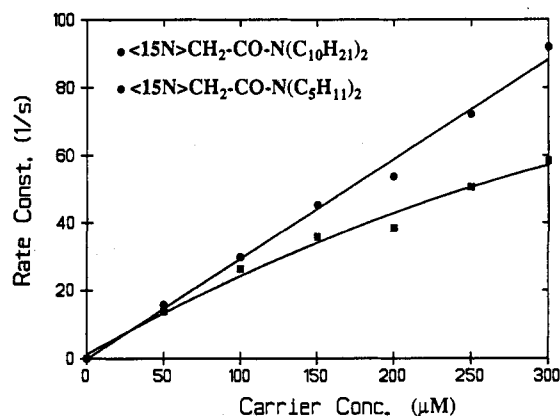


Figure 2. Typical plots show the dependence of the measured rate constants on the carrier concentration. Note the curvature present in the plot corresponding to $\langle 15\text{N} \rangle \text{CH}_2\text{CON}(\text{C}_5\text{H}_{11})_2$, which has been attributed to partial loss of the ligand to the surrounding aqueous environment; see text.

C_5H_{11} groups (see Figure 2), but even in those cases the functional relationship remains nearly linear. It is currently believed that those observations are the result of the reduced lipophilicity of these carriers relative to those containing $\text{C}_{10}\text{H}_{21}$ or $\text{C}_{18}\text{H}_{37}$ groups. Such reduced lipophilicity probably results in some loss of the carrier from the membrane into the aqueous environment. Current efforts are underway to find a model that fits these data.

It is evident from Table 1 that the order of Na^+ transport efficiency follows the expected ring size dependence, decreasing with the ring size in the order 18-membered rings $> 15 > 12$. Where comparisons were possible, no exceptions were found for this trend. Thus, $\langle 18\text{N} \rangle \text{CH}_2\text{CON}(\text{C}_n\text{H}_{2n+1})_2$ is always a better Na^+ transporter than the corresponding $\langle 15\text{N} \rangle$ analogue, which in turn is better than its $\langle 12\text{N} \rangle$ analogue. The same ring size dependence is also met by the corresponding secondary amide series. In general, these observations follow the trend of the corresponding homogeneous binding constants, determined in anhydrous methanol solution.¹⁷ However, a plot of the rate constant vs the homogeneous binding constant for all of the carriers studied resulted in a relatively high degree of scatter; see Figure 3. This scatter is somewhat improved if the carriers containing a secondary amide substituent are eliminated from the graph, hinting that there is something intrinsically different in the way that these systems bind and transport Na^+ across the vesicles.

One possible explanation for the different behavior between secondary and tertiary amides is the formation of hydrogen bonds

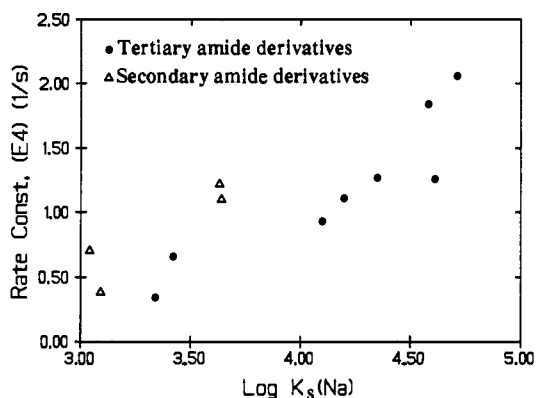


Figure 3. Plot of the normalized overall rate constants, k_2 , as a function of the logarithm of the stability constants determined in MeOH, $\log K_s$. Although a trend is visible, there is considerable scatter.

in the former.¹⁵⁻¹⁷ Such hydrogen bonding would lower the binding ability, especially if it occurs intramolecularly with the polyether ring oxygens. Intramolecular H-bond formation between the secondary amide hydrogen and the crown ether oxygens would inhibit complex formation by direct competition. Hydrogen bonding with the solvent, as suggested in ref 17, would result in the need to desolvate the side arm in order to complex the cation, at a cost of free energy. Since both types of H-bonds would result in a decrease of the cation-binding abilities of these ligands, direct experimental and theoretical evidence was sought to establish which of the two was responsible for the observations.

MMOD calculations²² were performed for two possible conformations of $(^{18}\text{N})\text{CH}_2\text{CONH}(\text{C}_5\text{H}_{11})$, one in which the amido hydrogen interacts with the macroring oxygens and the other where the carbonyl oxygen points to the polyether. Results showed that the conformation with the amido hydrogen close to the polyether was 57 kJ/mol more stable than the other conformation. The distance calculated between the amide nitrogen and the closest oxygens of the polyether ring in the stable structure was 3.3 Å. Therefore, the calculation indicates that this is a weak H-bond. Such bonds have been reported in other natural and synthetic molecules.^{23,24}

Definitive proof of the intramolecular nature of these H-bonds was obtained using ^1H NMR spectroscopy in CD_3CN . The amide proton resonances of these secondary amide carriers are observed to be downfield shifted relative to their normal position. For example, $(^{18}\text{N})\text{CH}_2\text{CONH}(\text{C}_{18}\text{H}_{37})$ has its amido hydrogen at 7.71 ppm, while it was expected around 7 ppm. Complexation of this compound with 1 equiv of Na^+ resulted in a pronounced upfield shift of the amido hydrogen resonance, to 6.63 ppm; see Figure 4. This is good evidence of H-bond breakage induced by cation binding with the polyether oxygens. In order to rule out the possibility that H-bonding involved the formation of intermolecular dimeric species, dilution experiments were conducted. ^1H NMR spectra were recorded for several of the secondary amides at two concentrations, 10 and 0.5 mM. The chemical shifts of the amido hydrogens remained exactly the same after dilution by this factor of 20. This is also evidence that the H-bond forms intramolecularly.

The conclusive NMR experiment was a homonuclear 2-D NOESY performed for all of the secondary amides at a concentration of 30 mM using a mixing time of 0.5 s. A NOESY spectrum is shown in Figure 5 for $(^{18}\text{N})\text{CH}_2\text{CONH}(\text{C}_{18}\text{H}_{37})$.

(22) MMOD calculations were conducted on a VAX 4000-600 in the University of Miami computer center. Parameters used for the MM2 force field were taken from Allinger's MM2 (85) program: Burkert, U.; Allinger, N. L. In *Molecular Mechanics*; American Chemical Society: Washington, DC, 1982.

(23) Koetzle, T. F.; Lehman, M. S. *The Hydrogen Bond*; Schuster, P., Zundel, G., Sandorfy, C., Eds.; North Holland Publishing Co.: Amsterdam, 1989.

(24) Topil, S.; Talbot, G. *J. Am. Chem. Soc.* **1990**, *112*, 8734.

Besides the expected cross peaks between the amido hydrogen and those in the side arm (1' and 2'), others appeared connecting the amido hydrogen with the polyether hydrogens at positions 1 and 2; see Figure 4 for the numbering scheme used. These experiments clearly established the intramolecular nature of H-bond formation of these secondary amide carriers.

Mechanistic Implications. In order to assess the mechanistic details of the transport process mediated by these carriers, a variable $[\text{Na}^+]$ study was done with one of the ligands. Since all of the compounds studied here constitute a very homogeneous family and since the availability of these synthetic materials is always low, only one compound was selected for this part of the work. The compound selected was $(^{15}\text{N})\text{CH}_2\text{CON}(\text{C}_{10}\text{H}_{21})_2$. Five different concentrations of $[\text{Na}^+]$ were chosen, ranging between 0.05 and 0.25 M, while keeping the carrier concentration constant at 100 μM . The values of the rate constants determined under these conditions are given in Table 2. A plot of $1/k$ vs $[\text{Na}^+]$ is shown in Figure 6 and was found to be reasonably linear. This observation, together with that previously noted about the linear relationship between the measured rate and the ligand concentration, strongly indicates that the transporting species is a 1:1 complex between the amide crown ether and Na^+ . This indicates that eq 3 applies, and thus from the ratio of the slope to the intercept of this plot it is possible to obtain the value of $K_s = 6.5$. As described above, K_s represents the stability constant for the complex in the membrane. Of the naturally-occurring ionophores that have been studied using similar NMR techniques by Riddell and his co-workers (M139603, monensin, nigericin, salinomycin, and narasin),⁵⁻⁹ salinomycin exhibits a very similar value of K_s with Na^+ , 6.1. Another similar value is that for monensin with K^+ , at 5.3.⁸ All of the other ionophores have larger K_s values with Na^+ , ranging from a high of 32.6 for monensin to a low of 11.0 for narasin.⁸ The value obtained for $(^{15}\text{N})\text{CH}_2\text{CON}(\text{C}_{10}\text{H}_{21})_2$ is thus perfectly consistent with those obtained for the naturally-occurring ionophores.

The most important mechanistic question that needs to be answered is whether the overall cation transport process across the membrane is limited by diffusion of the complex across the membrane ($k_{\text{diff}} \ll k_d$, eq 4), by dissociation of the complex ($k_d \ll k_{\text{diff}}$, eq 5), or by a competition between these two processes. As previously discussed, all naturally-occurring anionic ionophores studied by Riddell and his co-workers exhibit kinetic behavior controlled by slow complex dissociation, with diffusion across the membrane being fast and never rate limiting. This is in agreement with the anticipated behavior based on the fact that these naturally-occurring ionophores are anionic and thus form neutral complexes with the cations. Such neutral complexes have a highly lipophilic exterior and are thus able to effectively diffuse across the lipid bilayer environment, without the need for concomitant counteranion transport. The latter process is a difficult one, especially for hard and highly hydrophilic anions such as Cl^- . The need for the simultaneous transport of such an anion together with a cationic complex would certainly slow down diffusion across the membrane phase. This is the expected behavior for the synthetic ionophores presented here. The amide-containing crown ether ionophores can form relatively stable complexes with Na^+ in the membrane, as judged by the value of K_s presented above. But since the complex formed is positively charged, electroneutrality requirements dictate that an anion must be simultaneously transported.

The family of compounds presented here offers a unique opportunity to assess the relative kinetic importance of diffusion versus dissociation of the complex by direct comparison. Since the compounds containing C_5H_{11} substituents appear to be partially partitioned into the aqueous phase, *vide supra*, these will not be used for direct comparisons with those containing $\text{C}_{10}\text{H}_{21}$ or $\text{C}_{18}\text{H}_{37}$ in order to derive mechanistic conclusions. On the basis of dissociation rates measured for complexes of aza-

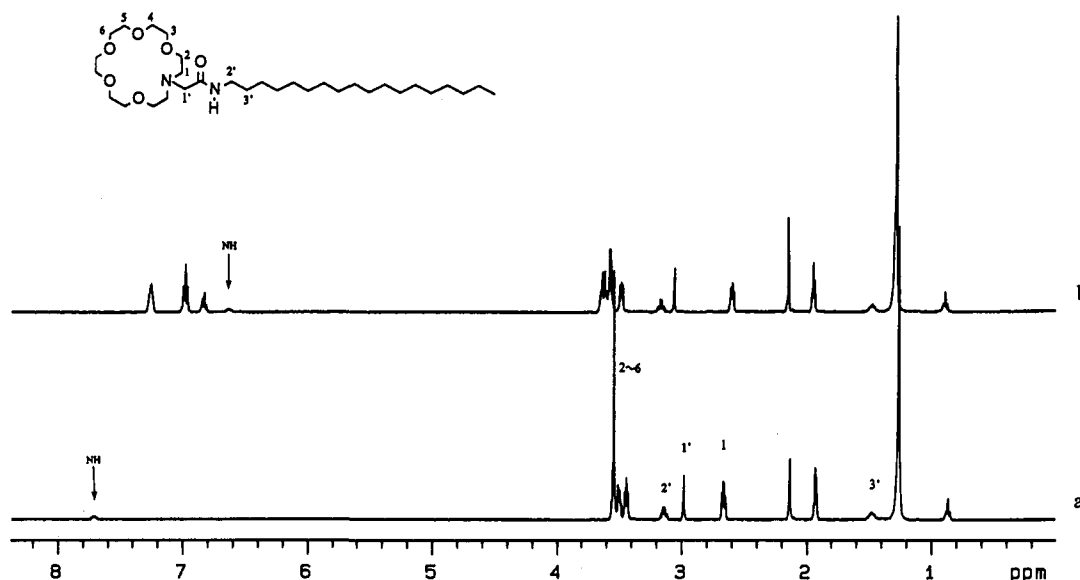


Figure 4. ^1H NMR spectra of (a) $(18\text{N})\text{CH}_2\text{CONHC}_3\text{H}_{11}$ and (b) its Na^+ complex in CD_3CN . Note the pronounced shift of the amidic proton resonance.

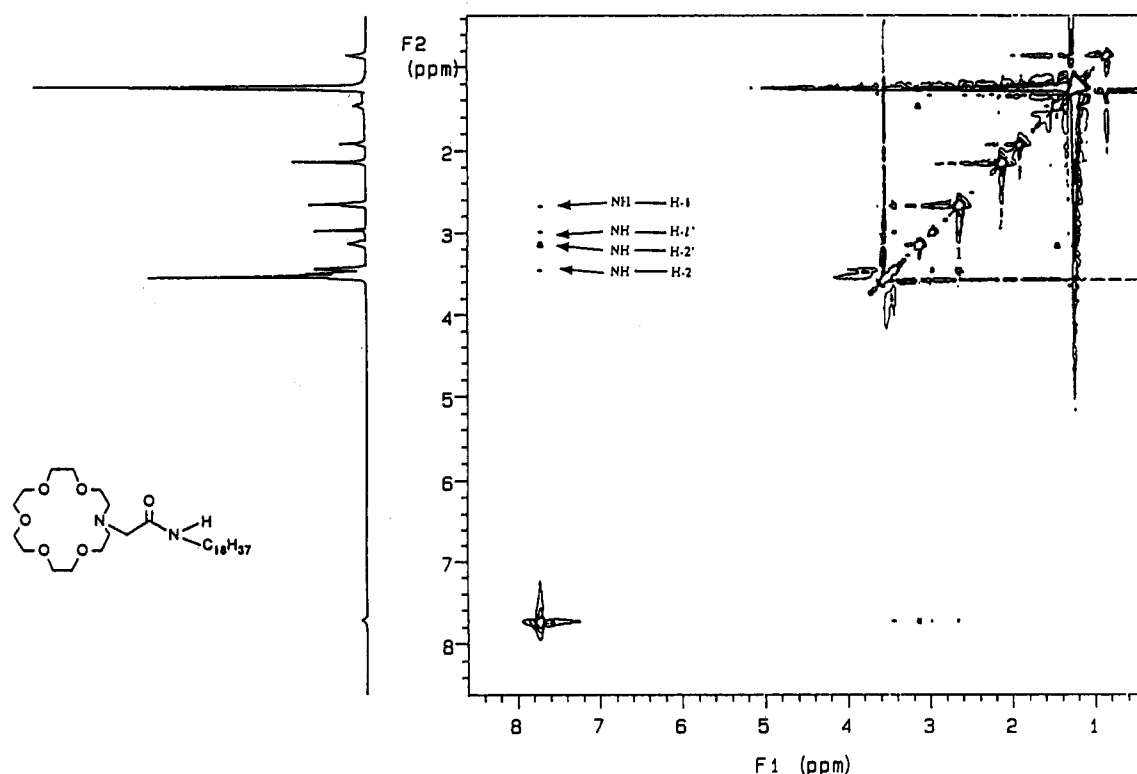


Figure 5. NOESY spectrum of $(18\text{N})\text{CH}_2\text{CONHC}_{18}\text{H}_{37}$ in CD_3CN . Correlation peaks are marked.

Table 2. Transport Rate Constants as a Function of $[\text{Na}^+]$

$[\text{Na}^+]$	$[\text{L}]_{\text{T}}(10^{-3})^a$	k (1/s)	$V_{\text{PG}} \%$	$V_{\text{PC}} \%$	$k_2^b(10^4)$	$1/k_2(10^{-4})$
0.05 M	3.2	42.4	17.9	14.7	1.60	0.63
0.10 M	3.2	30.8	20.4	14.7	1.32	0.76
0.15 M	3.2	24.5	18.5	14.7	0.96	1.05
0.20 M	3.2	20.1	21.7	14.7	0.92	1.09
0.25 M	3.2	16.0	23.8	14.7	0.80	1.24

^a $[\text{L}]_{\text{T}} = [(\text{15N})\text{CH}_2\text{CON}(\text{C}_{10}\text{H}_{21})_2]/[\text{PC}]$, $[(\text{15N})\text{CH}_2\text{CON}(\text{C}_{10}\text{H}_{21})_2] = 100 \mu\text{M}$, $[\text{PC}] = 0.031 \text{ mM}$. ^b Normalized transport rate constant $k_2 = (k/[\text{L}]_{\text{T}}) \times (V_{\text{PG}}\%/V_{\text{PC}}\%)$; its units are $[\text{mol lipid} \cdot (\text{mol carrier})^{-1} \cdot \text{s}^{-1}]$.

crown ether complexes in homogeneous solution, it seems reasonable to assume that the cation dissociation rates for complexes containing the same crown ether ring size and the same amide substituent situated in the same relative position

relative to the ring should be very similar.²⁵ Therefore, if the rate of dissociation of the complexes was the rate-determining step in the overall transport processes measured here, little difference would be anticipated for those complexes containing the same crown ring. This is clearly not the case. Note for example that the ligands containing $\text{C}_{10}\text{H}_{21}$ are always better transporters than those containing $\text{C}_{18}\text{H}_{37}$, as long as the same macrocyclic ring is present. This holds true even in the case of the secondary amide compounds. The fact that the lower molecular mass complexes (containing $\text{C}_{10}\text{H}_{21}$ substituents) are more effective transporters than their higher mass analogues is also a good indication that the differences are the result of a diffusion process. The fact that the C_5H_{11} -substituted analogues are not even better transporters than those with $\text{C}_{10}\text{H}_{21}$ is simply due to the partial loss of the

(25) Izatt, R. M.; Pawlak, K.; Bradshaw, J. S. *Chem. Rev.* **1991**, *91*, 1721.

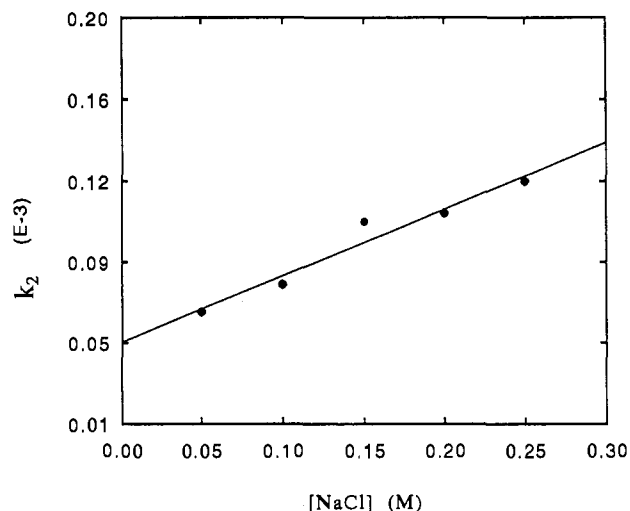


Figure 6. Plot showing the effect of varying the $[\text{Na}^+]$ on the value of k_2 . The linear correlation is indicative of the formation of a 1:1 complex in the membrane.

former to the aqueous environment. The conclusion is that the overall cation transport mechanism is being controlled by the diffusion of the complex across the bilayer membrane of the LUVs. This is not surprising in view of the fact that these amide-substituted ligands do not have a negative charge and are not able to shield the cation as effectively as the naturally-occurring ionophores. The latter are able to wrap around the cation very effectively, resulting in a very lipophilic neutral complex.

Another indirect proof that the rate-limiting step is diffusion across the membrane can be obtained if the opposite situation is assumed. Thus, if dissociation is assumed to be rate determining, eq 5 would apply and the slope of Figure 6 would yield a value of k_d of $0.64 \times 10^4 \text{ M s}^{-1}$. Also, a value of k_f of $4.2 \times 10^4 \text{ s}^{-1}$ would result from the intercept. Both of these values are larger than the corresponding ones for salinomycin- Na^+ ,⁸ a situation that would necessarily lead to more efficient transport by the synthetic ligand if k_d is the rate-limiting step. Since salinomycin actually exhibits an overall transport rate constant, k_2 , of $1.6 \times 10^4 \text{ s}^{-1}$,⁸ which is larger than that of $(15\text{N})\text{CH}_2\text{CON}(\text{C}_{10}\text{H}_{21})_2$, the process cannot be controlled by k_d . This reasoning by negative inference, together with the arguments in the previous paragraph, provides strong evidence that the overall Na^+ transport rate is controlled by slow diffusion of the complexes across the membrane phase.

Since diffusion is rate limiting ($k_{\text{diff}} \ll k_d$), eq 4 applies under the present conditions. From the slope of the plot in Figure 6 it was possible to calculate the diffusion rate constant, k_{diff} . The

value obtained was $3.2 \times 10^3 \text{ s}^{-1}$. It should be pointed out that the value of k_d determined by Riddell and his co-workers for monensin- Na^+ was $1.5 \times 10^3 \text{ M s}^{-1}$. It may initially seem that these results are contradictory with those previously presented where the overall Na^+ transport efficiency was said to be comparable for both of these carriers; see Table 1. It might be inferred then that the k_d value for monensin- Na^+ would have to be equal to the k_{diff} for $(18\text{N})\text{CH}_2\text{CON}(\text{C}_{10}\text{H}_{21})_2\text{-Na}^+$, since these are the rate-determining steps involved for these two carriers. This is easily accounted for if one remembers that the rate constant for the overall transport efficiency (k_2) also depends on the value of the stability constant; see eq 3. The value of K_1 for monensin- Na^+ is 32.6, thus compensating for the lower k_d value compared to the k_{diff} value for the crown carrier.

Conclusions

Twelve synthetic lipophilic crown ethers containing an amide substituent were evaluated for their Na^+ transport ability in large unilamellar vesicles using ^{23}Na NMR spectroscopy. This is the first time that such a systematic set of synthetic ionophores has been investigated in a lipid bilayer environment. It is also the first time that a mechanistic study has been conducted to establish the slow step controlling the overall Na^+ transport efficiency mediated by these neutral ionophores.

Overall transport rates were observed to be surprisingly high, with one particular synthetic ionophore exhibiting a value comparable to that of a naturally-occurring ionophore, monensin. The value for the overall rate constant was $2.1 \times 10^4 \text{ s}^{-1}$ for $(18\text{N})\text{CH}_2\text{CON}(\text{C}_{10}\text{H}_{21})_2\text{-Na}^+$ and $2.0 \times 10^4 \text{ s}^{-1}$ for momensin- Na^+ .

In general, transport rates followed the expected trend based on the size of the crown ether ring present in the carrier ligand. The order was always $18 > 15 > 12$. For the compounds containing a secondary amide, Na^+ binding and transport was not as efficient as for the tertiary analogues. Using NOESY, it was conclusively shown that the secondary amides exhibit intramolecular H-bonding between the amidic hydrogen and the crown ring, thus inhibiting binding and consequently transport.

The overall transport process is controlled by diffusion of the complex across the bilayer. This is in direct contrast to the observed behavior for cation transport mediated by anionic naturally-occurring ionophores, for which the process is always controlled by dissociation of the complex. To our knowledge this is the first time that the mechanism of cation transport mediated by a synthetic ionophore has been determined in a bilayer medium.

Acknowledgment. The authors express their gratitude to the NIH (Grant GM-33940) and to the NSF (Grant DMR-9119986) for partial support of this work.